Spontaneous Transformation from Micelle to Vesicle Associated with Sequential Conversions of Comprising Amphiphiles within Assemblies

Katsuto Takakura[a,*], Takahiro Yamamoto[a], Kensuke Kurihara[b], Taro Toyota[b,c], Kiyoshi Ohnuma[d], and Tadashi Sugawara[c,e,**]

[a] Department of Chemistry and Biochemistry, Suzuka National College of Technology, Shiroko-cho, Suzuka, Mie 510-0294, Japan, [b] Department of Basic Science, Graduate School of Arts and Sciences, The University of Tokyo, 3-8-1 Komaba, Meguro-ku, Tokyo 153-8902, Japan, [c] Research Center for Complex Systems Biology, The University of Tokyo, 3-8-1 Komaba, Meguro-ku, Tokyo 153-8902, Japan, [d] Top Runner Incubation Center for Academia-Industry Fusion, Nagaoka University of Technology, 1603-1 Kamitomioka-cho, Nagaoka, Niigata 940-2188, Japan, [e] Department of Chemistry, Faculty of Science, Kanagawa University, 2946 Tsuchiya, Hiratsuka, Kanagawa 259-1293, Japan

Supplementary Information

Table of content

Experimental details

General. All commercially available reagents were purchased from Tokyo Kasei Co. or Wako Pure Chemical Co. and were used without further purification. ^{1}H NMR spectra were recorded on a JEOL JNM-A400 spectrometer. High-resolution electrospray ionization mass spectra (HRMS-ESI) were recorded on an Applied Biosystems QSTAR-Elite spectrometer with a monosodium adduct of dibutylphthalate ($C_{16}H_{22}NaO_4$, exact mass: 301.1416) for $\mathbf{N_1}$ and $\mathbf{N_2}$ or a monoproton adduct of reserpine ($C_{33}H_{41}N_2O_9$, exact mass: 609.2821) for **V** as the internal standard. The dynamic behavior of the vesicles was monitored with OLYMPUS IX71 (obj. lens × 100) and OLYMPUS BX51 (obj. lens × 40) equipped with an image-recording and image-processing system.

[2-[4-(2-Dodecylazomethinyl)phenoxy]ethyl}trimethylammonium bromide ($\mathbf{N_1}$).
[2-(4-Formylphenoxy)ethyl]trimethylammonium bromide **E** (2.88 g, 10.0 mmol), which was prepared following the procedure described in the literature (K. Takakura, T. Sugawara, *Langmuir*, 2004, **20**, 3832.), and *n*-dodecylamine (1.85 g, 10.0 mmol) were dissolved in absolute ethanol (50 mL), and a catalytic amount of acetic acid was added. The mixture was refluxed for 12 h and then cooled. After the evaporation of ethanol, the residue was washed with acetone to afford the amphiphilic imine derivative $\mathbf{N_1}$ as a colorless crystal (2.51 g, 80.3%).

δ_H (400 MHz,$CDCl_3$; Me_4Si) 0.85 (3H, t, *J*= 6.95 Hz, CH_3), 1.18-1.75 (20H, m, -$(CH_2)_{10}$-), 3.57 (9H, 2H, t, s, *J*= 7.07 Hz, NMe_3, -N-$\underline{CH_2}$-CH_2-O-), 4.32 (2H, t, *J* =4.51 Hz, -$\underline{CH_2}$-O-), 4.52 (2H, s, -$\underline{CH_2}$-N=CH-), 6.94 (2H, d, *J* =8.78 Hz, H_o), 7.67 (2H, d, *J* = 8.78 Hz, H_m), 8.18 (1H, s, -N=$\underline{CH}$-),

δ_C (100 MHz,$CDCl_3$; Me_4Si) 14.2 (-CH_3), 22.8-32.0 (10 peaks, -$(CH_2)_{10}$-), 54.9 (-$N(CH_3)_3$), 61.8 (-$\underline{CH_2}$-N=CH-), 62.5 (-N-$\underline{CH_2}$-CH_2-O-), 65.1 (-N-CH_2-$\underline{CH_2}$-O-), 114.5 (C_o), 129.9 (C_p), 131.0 (C_m), 158.6 (-N=$\underline{CH}$-), 159.6 (C_{ipso}).

HRMS-ESI-TOF (*m*/*z*): $[M\text{-}Br]^+$ calcd for $C_{24}H_{43}N_2O$, 375.3369; found 375.336.

Dodecyl[2-(4-formylphenoxy)ethyl]dimethylammonium bromide ($\mathbf{N_2}$). 4-(2-Bromoethoxy)benzaldehyde (2.29 g, 10.0 mmol), which was prepared following the procedure described in the literature,(Y. Okahata, T. Kunitake, *J. Am. Chem. Soc.*, 1979, **101**, 5331.) was dissolved in *N*, *N*-dimethyldodecylamine (10 mL) and the solution was heated at 80 °C for 24 h. The reaction mixture was washed with diethyl ether at room temperature and the resulting powder was recrystallized from chloroform/*n*-hexane to afford the amhiphilic aldehyde $\mathbf{N_2}$ as a colorless crystal (2.74 g, 82.0%) .

δ_H (400 MHz,$CDCl_3$; Me_4Si) 0.85 (3H, t, *J* =6.80 Hz, -CH_3) , 1.18-1.80 (20H, m, -$(CH_2)_{10}$-), 3.51 (6H, s, $N(CH_3)_2$), 3.63 (2H, m, -O-CH_2-$\underline{CH_2}$-N^+-), 4.31 (2H, t, *J* =4.2 Hz, -N-$\underline{CH_2}$-$C_{11}H_{21}$), 4.63 (2H, t, *J* =4.2 Hz, -O-$\underline{CH_2}$-CH_2-N), 7.04 (2H, d, *J* =8.78 Hz, H_o), 7.83 (2H, d, *J* =6.83 Hz, H_m), 9.86 (1H, s, -CHO).

δ_C (100 MHz,$CDCl_3$; Me_4Si) 13.0 (-CH_3) , 22.8-32.0 (10 peaks,-$(CH_2)_{10}$-), 52.7 (-$N(CH_3)_2$), 62.8, 62.5 (-O-CH_2-$\underline{CH_2}$-N^+-, -N-$\underline{CH_2}$-$C_{11}H_{21}$), 66.3 (-O-$\underline{CH_2}$-CH_2-N^+-), 115.0 (C_o), 131.2 (C_p), 132.3 (C_m), 161.8 (C_{ipso}), 190.8 (-CHO).

HRMS-ESI-TOF (*m/z*): $[M\text{-}Br]^+$ calcd for $C_{23}H_{40}NO_2$, 362.3053; found 362.3057.

Dodecyl{2-[4-(2-dodecylazomethinyl)phenoxy]ethyl}dimethylammonium bromide (V). Compound $\mathbf{N_2}$ (0.221 g, 0.5 mmol) and dodecylamine (0.186 g, 1.00 mmol) were dissolved in absolute ethanol (5 mL), and a catalytic amount of acetic acid was added. The mixture was refluxed for 12 h and then cooled. After the evaporation of ethanol, the residue was washed with diethyl ether to afford the amphiphilic imine **V** as a colorless crystal (0.261 g, 85.6%).

δ_H (400 MHz,$CDCl_3$; Me_4Si) 0.85 (6H, t, J = 6.4 Hz, CH_3), 1.18-1.65 (40H, m, $CH_3(\underline{CH_2})_{10}CH_2$-N=, $CH_3(\underline{CH_2})_{10}CH_2$-$N^+$-), 3.45-3.64 (8H, m, -$N^+(\underline{CH_3})_2\underline{CH_2}(CH_2)_{10}CH_3$), 4.30 (2H, t, J =4.2Hz, -O-CH_2-$\underline{CH_2}$-N^+-), 4.52 (2H, t, J =4.0 Hz, -O-$\underline{CH_2}$-CH_2-N^+-), 6.90 (2H, d, J =8.40 Hz, H_o), 7.67 (2H, br, H_m), 8.18 (1H, s, -N=$\underline{CH}$-).

δ_C (100 MHz,$CDCl_3$; Me_4Si) 14.2 (-CH_3), 22.8-32.0 ($CH_3(\underline{CH_2})_{10}CH_2$-N, $CH_3(\underline{CH_2})_{10}$ CH_2-N^+-), 52.1 (-$N(CH_3)_3$), 61.8 (-$\underline{CH_2}$-N=CH-), 62.5, 62.4 (-N^+-$\underline{CH_2}$-CH_2-O-, -N^+-$\underline{CH_2}$-$(CH_2)_{10}CH_3$), 66.3(-O-$\underline{CH_2}$-CH_2-N^+-), 114.5(C_o), 130.0 (C_p), 130.9 (C_m), 158.7(C_{ipso}), 159.6 (-N=$\underline{CH}$-).

HRMS-ESI-TOF (*m/z*): $[M\text{-}Br]^+$ calcd for $C_{35}H_{65}N_2O$, 529.5091; found 529.5075.

^{1}H NMR Spectroscopic Monitoring of the Formation of Amphiphilic Imine V. An equimolar mixture of amphiphilic precursors $\mathbf{N_1}$ and $\mathbf{N_2}$ was dissolved in dried $CHCl_3$. After the evaporation of $CHCl_3$, the residual mixture was dissolved in D_2O to prepare a solution (10.0 mM for each). Immediately after the preparation of the D_2O solution, its ^{1}H NMR spectra were measured every 10 min on a JEOL JNM-A400 spectrometer at room temperature (25 °C). The conversion from $\mathbf{N_1}$ and $\mathbf{N_2}$ to vesicular membrane lipid **V** and the molar fraction of each component were monitored on the basis of the ratio of the signal area of components to the starting material.

Optical Microscopy Observation. Amphiphilic precursors $\mathbf{N_1}$ and $\mathbf{N_2}$ were dissolved in dried $CHCl_3$. After the evaporation of $CHCl_3$, the residual mixture was dissolved in deionized water to prepare an aqueous solution. The $\mathbf{N_1}$ solution was mixed with that of $\mathbf{N_2}$ in equivalent volumes and the mixed solution (20 μL, 10 mM for each) was immediately placed on a glass plate and the plate was covered with a cover glass at room temperature. The phase contrast or differential interference contrast microscopy images of the aggregates in the solution were recorded using OLYMPUS IX71 (obj. lens × 100) and OLYMPUS BX51 (obj. lens × 40) equipped with an image-recording and image-processing system.

Optical Microscopy Observation of Giant Vesicles Prepared by the Film Swelling Method. The mixture composed of sets of $\mathbf{N_1}$ (2.3 mg), $\mathbf{N_2}$ (2.1 mg), **V** (27.4 mg) and **E** (15.8 mg) was dissolved in dried CH_2Cl_2. After evaporating the solvent, the residual mixture was dissolved in 10.0 mL of deionized water. The dispersion was immediately placed on a glass plate and the plate was covered with a cover glass. The phase contrast microscopy images of GVs were recorded using an OLYMPUS IX71 (obj. lens × 100) equipped with an image-recording and image-processing system at room temperature.

Dynamic Light Scattering (DLS) Measurement. A dispersion was prepared by evaporating a chloroform solution of $\mathbf{N_1}$ (22.8 mg) or $\mathbf{N_1}$ (21.4 mg) under reduced pressure and dispersing the residue with 10 mL of milliQ water (10 mM, respectively). The light counting time was 600 s and each size distribution was obtained as an average of three determinations using NIKKISO MicroTrac UPA150. For mixed micelles, after evaporating a mixed solution of $\mathbf{N_1}$ (45.5 mg) and $\mathbf{N_2}$ (42.8 mg) and dispersing with milliQ water (10 mM for each), the dispersion was measured by the same procedure above.

Spectral charts of synthetic amphiphiles N_1, N_2, and V

^{1}H NMR spectra of $\mathbf{N_1}$, $\mathbf{N_2}$, and **V** are shown in figures S1, S2, and S3, respectively.

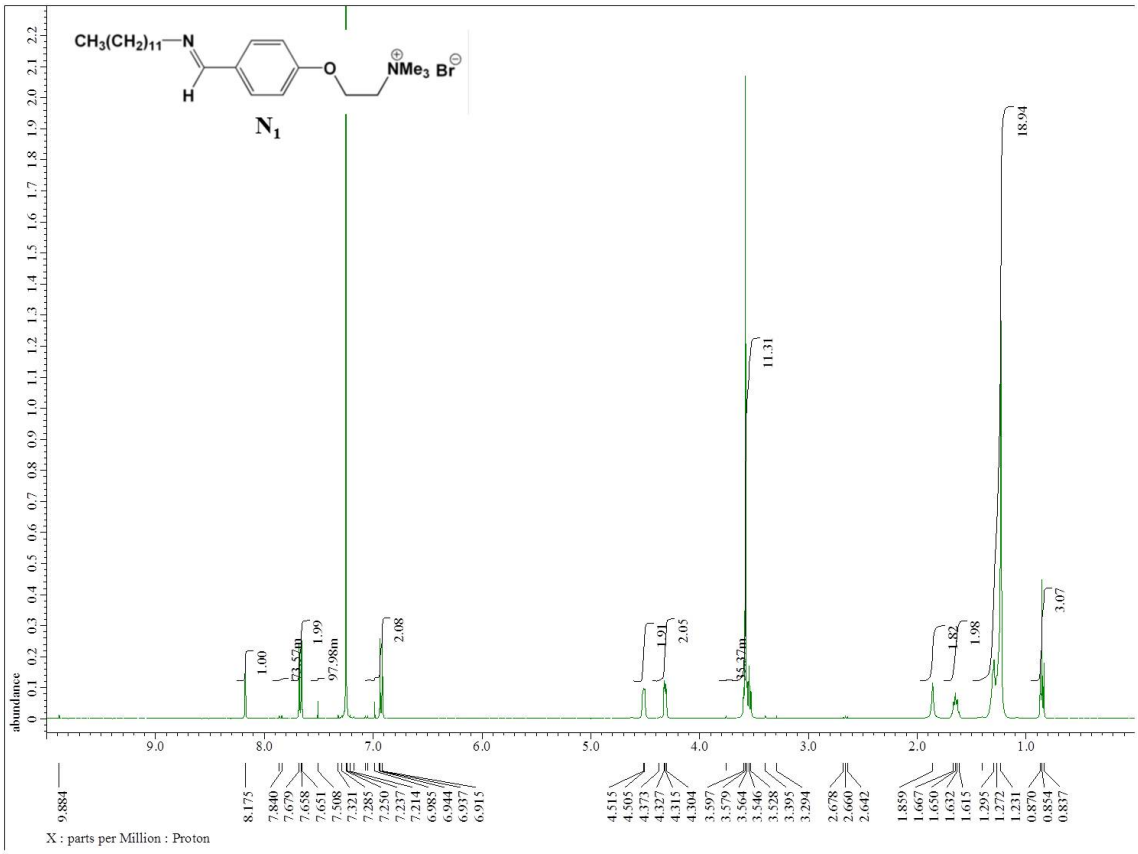

Figure S1. ^{1}H NMR spectra of compound $\mathbf{N_1}$ ($CDCl_3$ solution).

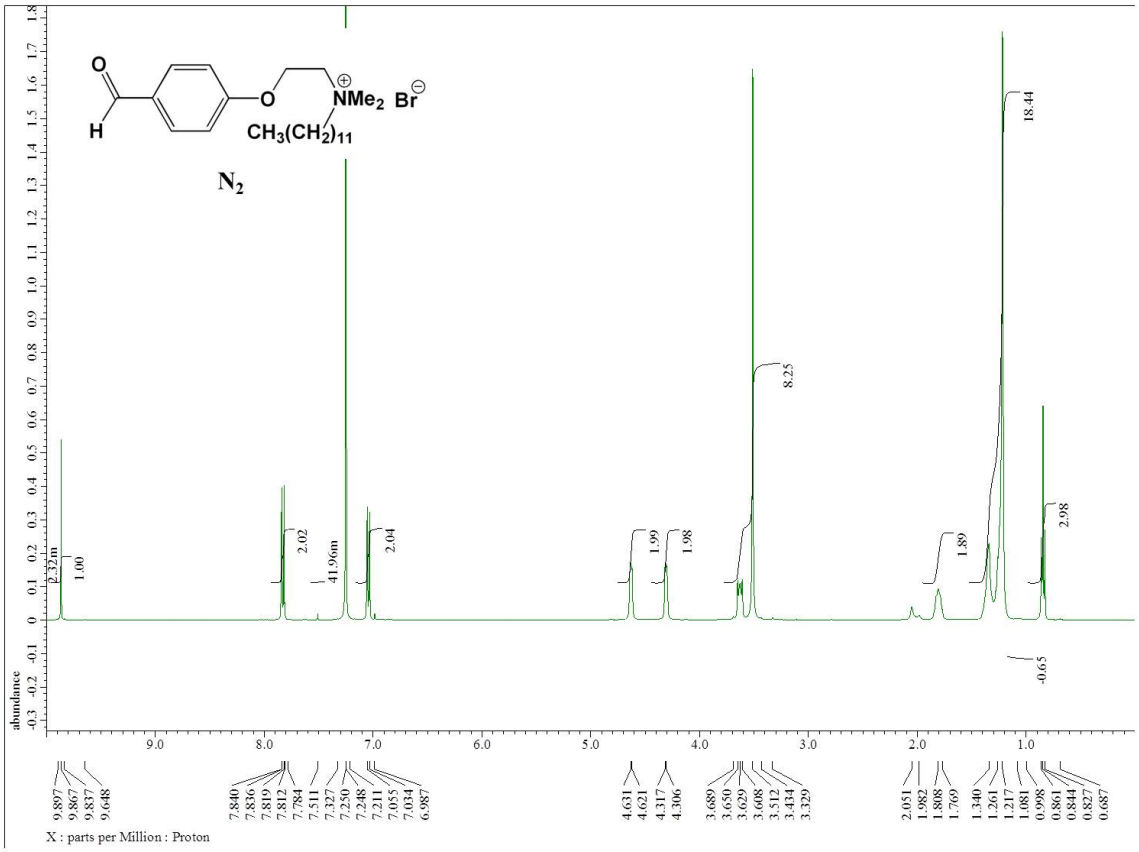

Figure S2. ^{1}H NMR spectra of compound $\mathbf{N_2}$ ($CDCl_3$ solution).

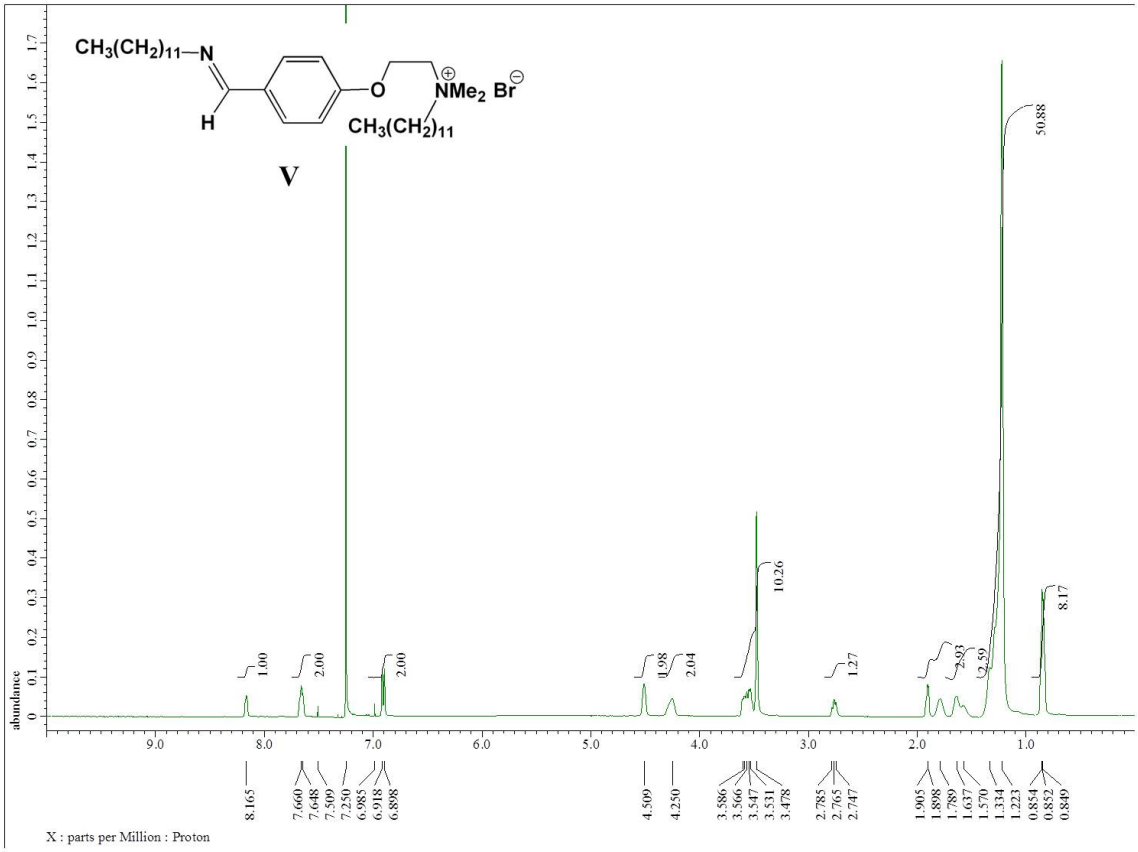

Figure S3. ^{1}H NMR spectra of compound **V** ($CDCl_3$ solution).

^{13}C NMR spectra of **N_1**, **N_2**, and **V** are shown in figures S4, S5, and S6, respectively.

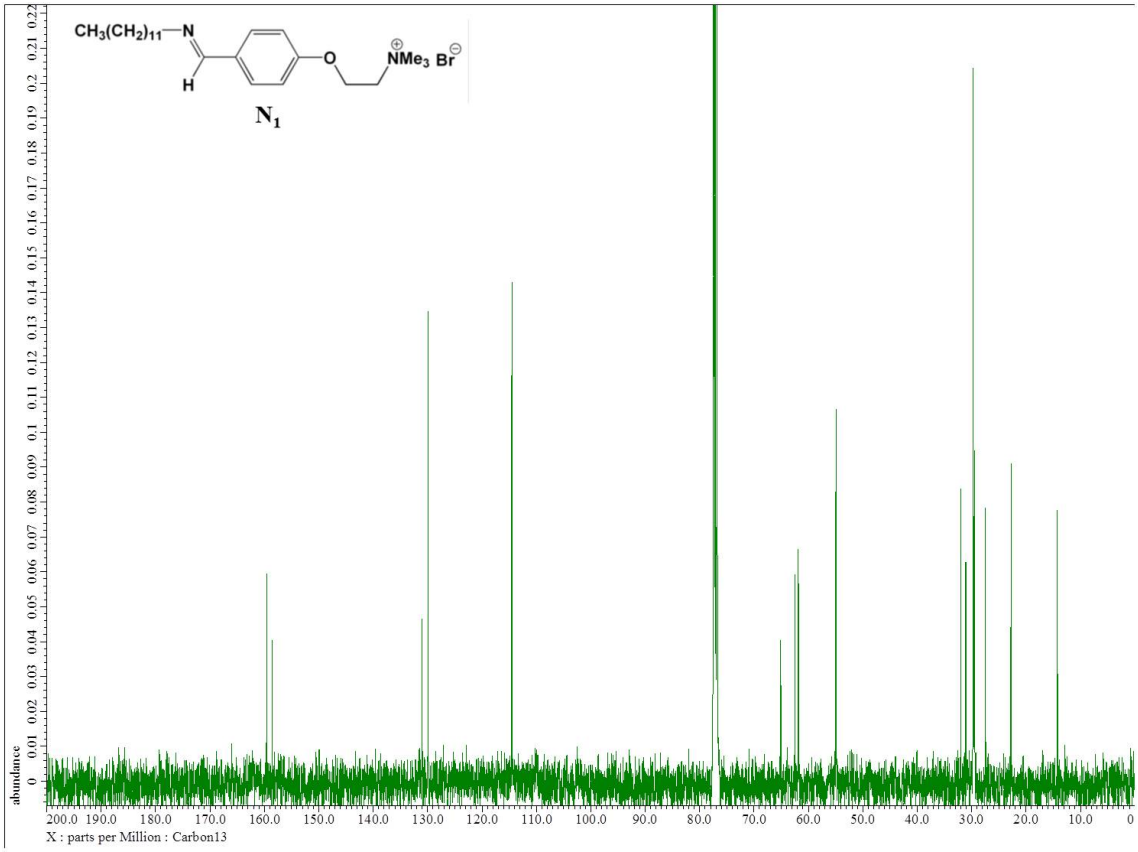

Figure S4. ^{13}C NMR spectra of compound **N_1** ($CDCl_3$ solution).

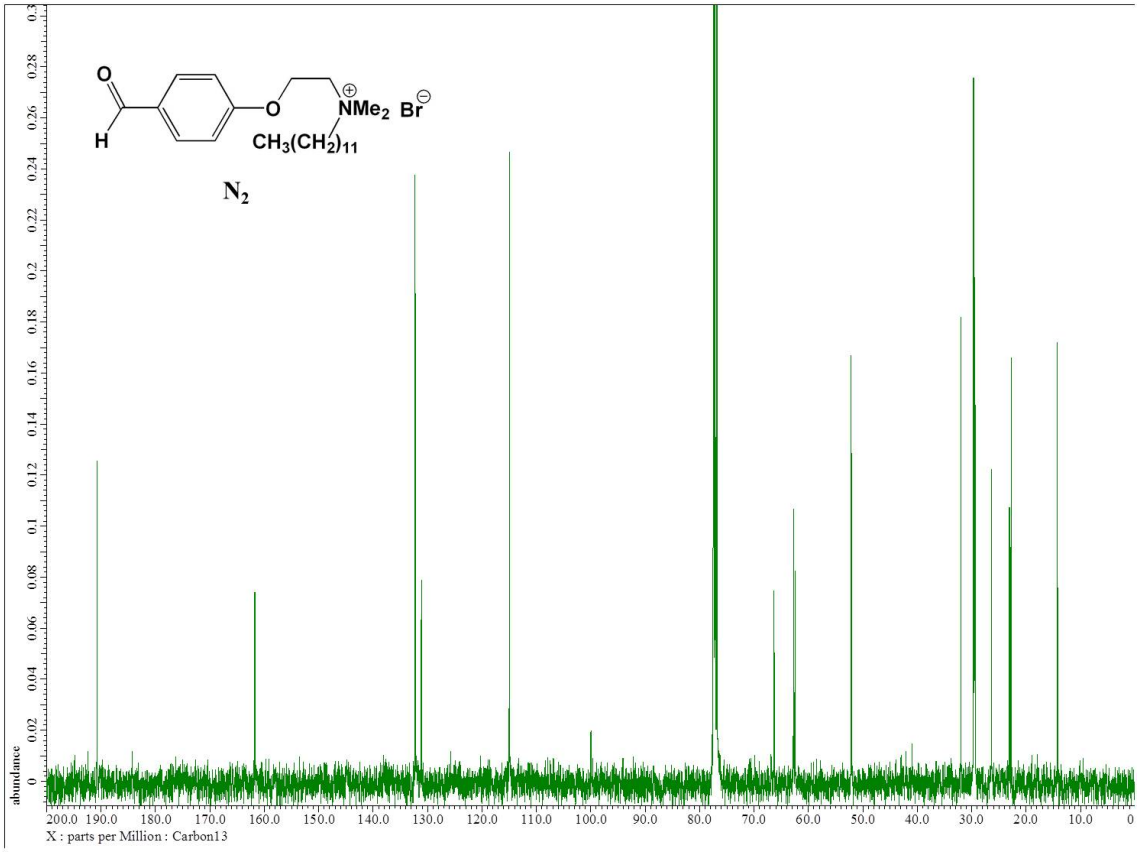

Figure S5. ^{13}C NMR spectra of compound $\mathbf{N_2}$ ($CDCl_3$ solution).

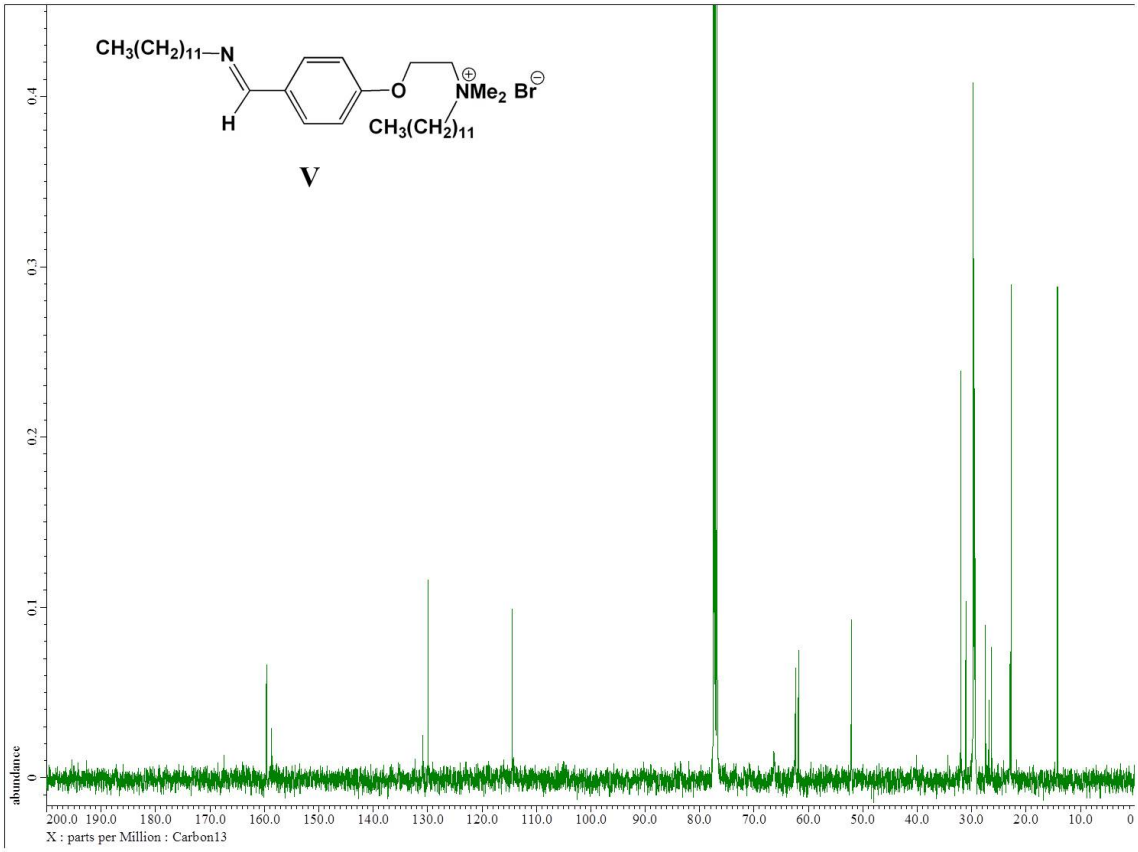

Figure S6. ^{13}C NMR spectra of compound **V** ($CDCl_3$ solution).

High-resolution ESI-TOF mass spectra of $\mathbf{N_1}$, $\mathbf{N_2}$, and **V** are shown in figures S7, S8, and S9, respectively.

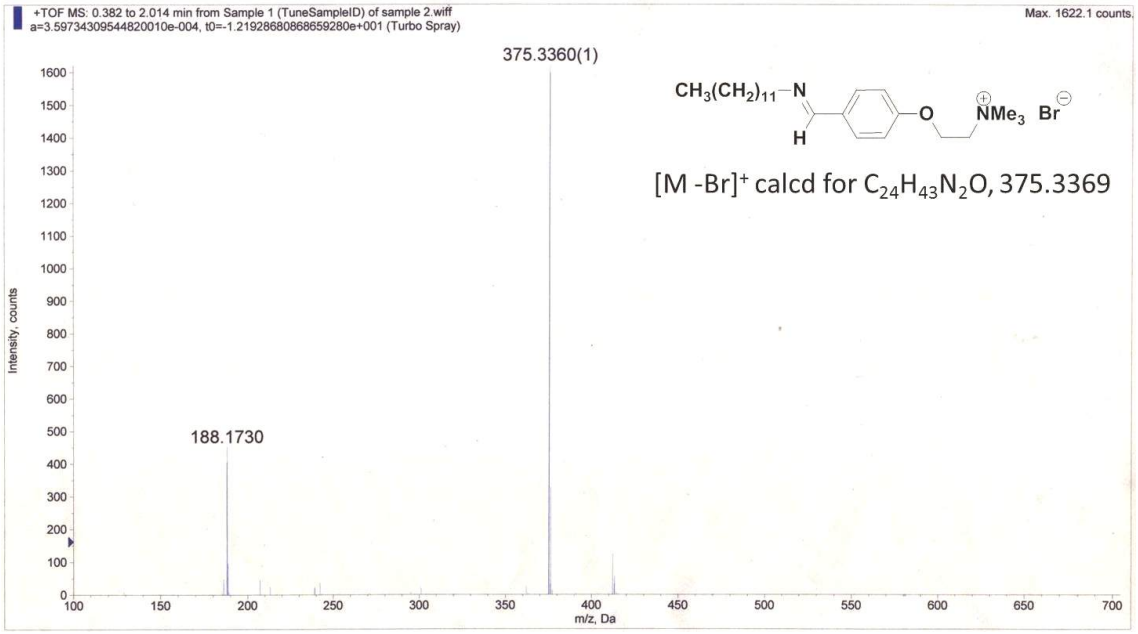

Figure S7. ESI-TOF Mass spectra of compound $\mathbf{N_1}$.

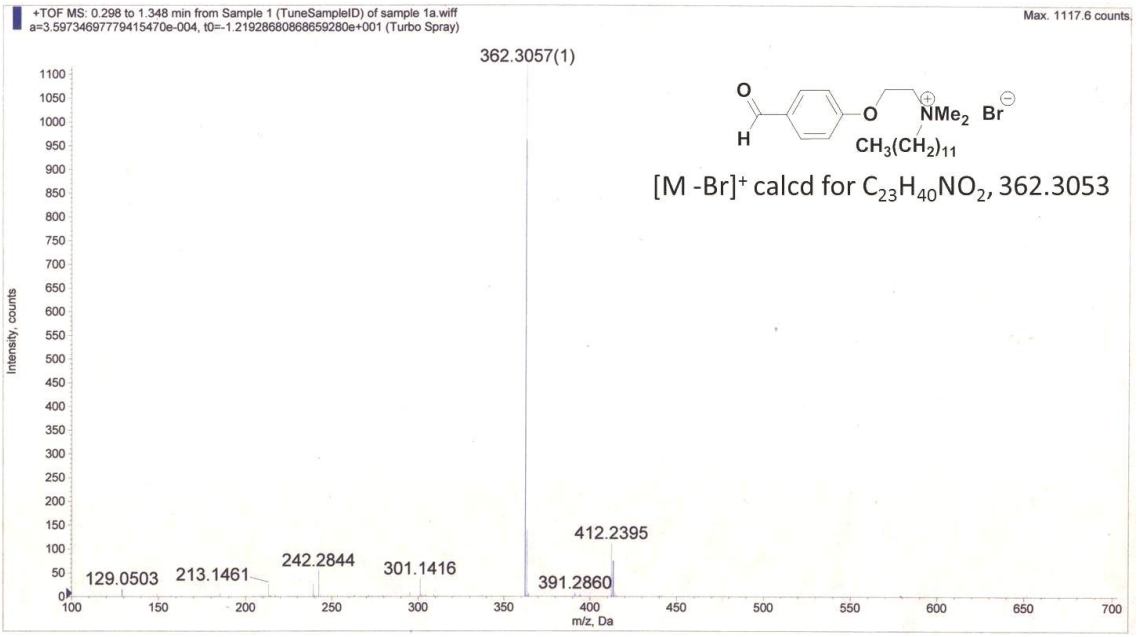

Figure S8. ESI-TOF Mass spectra of compound $\mathbf{N_2}$.

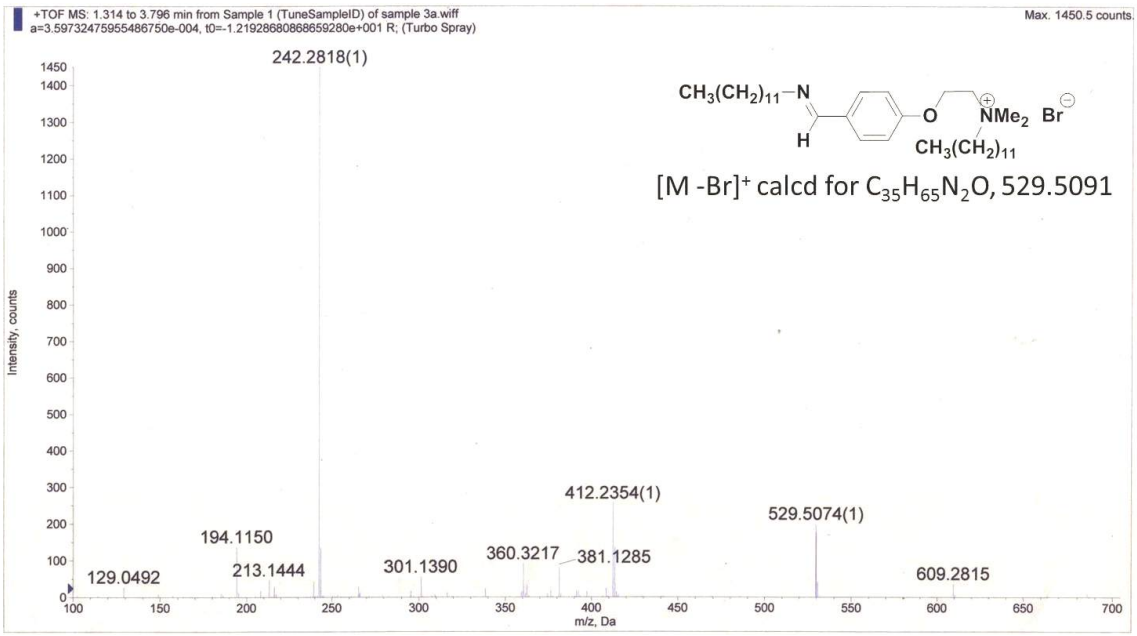

Figure S9. ESI-TOF Mass spectra of compound **V**.

The ^{1}H NMR spectral change of the equimolar mixture of $\mathbf{N_1}$ and $\mathbf{N_2}$ every 120 min at 25 °C is shown in Fig. S10. In compensation for the decrease in the intensities of signals assigned to $\mathbf{N_1}$ and $\mathbf{N_2}$, signals assigned to the product **V** and **E** increased in intensity. Whereas signals of $\mathbf{N_1}$, $\mathbf{N_2}$ and **V** gradually broadened, signals of electrolyte **E** remained sharp. The result suggests that the assembly composed of amphiphiles ($\mathbf{N_1}$, $\mathbf{N_2}$, **V**) grew in size (C. R. Sanders. *Prog. NMR Spectrosc.,* 1994, **26**, 421.), whereas electrolyte **E** was monodispersed in water. The reason for the broadening of the signals of $\mathbf{N_1}$ and $\mathbf{N_2}$ may be explained by the slowing down of tumbling motions of these amphiphiles in the assembly, the size of which increased due to the generation of **V**.

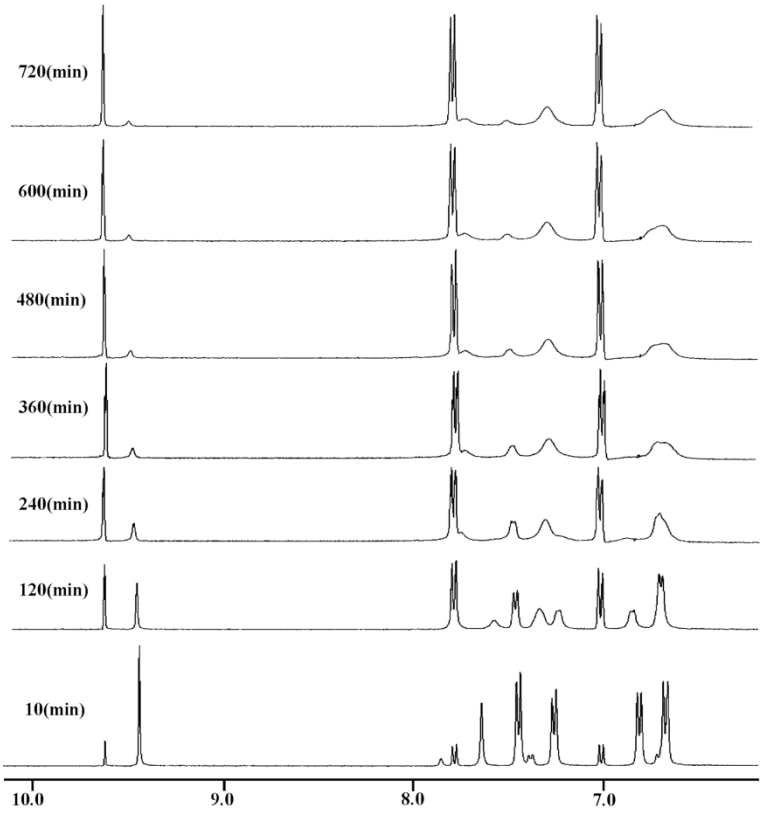

Figure S10. ^{1}H NMR spectral change in D_2O solution of $\mathbf{N_1}$ and $\mathbf{N_2}$ (10 mM) at 25°C. The signals were assigned as follows: δ = 9.64 ($\mathbf{N_1}$, -CHO, 1H), 9.46 (**E**, -CHO, 1H), 7.87(**V**, -CH=N, 1H), 7.80 (**V**, $H_{2,6}$, 2H), 7.66 ($\mathbf{N_1}$, -CH=N, 1H), 7.46 ($\mathbf{N_2}$, $H_{2,6}$, 2H), 7.40 (**V**, $H_{2,6}$, 2H), 7.27 ($\mathbf{N_1}$, $H_{2,6}$, 2H), 7.02 (**V**, $H_{3,5}$, 2H), 6.82 ($\mathbf{N_1}$, $H_{3,5}$, 2H), 6.69 (**V**, $H_{3,5}$, 2H).

Introduction of the equations expressing molar fractions of each component consisting of aggregates from ^{1}H NMR signal areas

When the area of the molar amounts of $\mathbf{N_1}$, $\mathbf{N_2}$, **V**, **E** and dodecylamine (**A**) are defined as n_1, n_2, v, e and a, respectively, the ratio among areas of ^{1}H NMR signals at 9.77 ppm, at 9.59 ppm and in the range from 6.60 ppm to 8.20 ppm (A_1, A_2, A_3, respectively) is expressed as equation (1).

$$A_1 : A_2 : A_3 = e : n_2 : 5n_1 + 4n_2 + 5v + 4e \qquad (1)$$

Since transamination from $\mathbf{N_1}$ to $\mathbf{N_2}$ is regarded as a sequence of hydrolysis of $\mathbf{N_1}$ ($\mathbf{N_1} + H_2O \rightarrow \mathbf{A} + \mathbf{E}$) and dehydrocondensation between $\mathbf{N_2}$ and **A** ($\mathbf{N_2} + \mathbf{A} \rightarrow \mathbf{V} + H_2O$), equation (2) can be obtained.

$$e = a + v \qquad (2)$$

Furthermore, equations (3) and (4) are obtained because the molar amounts of $\mathbf{N_1}$ and $\mathbf{N_2}$ are equal initially. The symbol n_0 indicates the molar amounts of both $\mathbf{N_1}$ and $\mathbf{N_2}$ at the initial stage of reaction.

$$n_0 = n_1 + e \qquad (3)$$
$$n_0 = n_2 + v \qquad (4)$$

From these four equations, the ratio of molar amounts among molecules contained in aggregates can be derived as follows.

$$n_1 : n_2 : v : a = -9A_1 + A_2 + A_3 : 10A_2 : A_1 - 9A_2 + A_3 : 9A_1 + 9A_2 - A_3 \qquad (5)$$

Therefore, molar fractions of $\mathbf{N_1}$, $\mathbf{N_2}$, **V** and dodecylamine in aggregates, which are defined as x_1, x_2, x_v and x_a, respectively, are expresses as equation (6)-(9).

$$x_1 = (-9A_1 + A_2 + A_3) / (A_1 + 11A_2 + A_3) \qquad (6)$$
$$x_2 = 10A_2 / (A_1 + 11A_2 + A_3) \qquad (7)$$
$$x_v = (A_1 - 9A_2 + A_3) / (A_1 + 11A_2 + A_3) \qquad (8)$$
$$x_a = (9A_1 + 9A_2 - A_3) / (A_1 + 11A_2 + A_3) \qquad (9)$$

The conversion rate (%) of the migration is described as equation (10).

conversion rate (%) = $100x_v/(x_1 + x_a + x_v)$ (10)

Dynamic light scattering measurement of morphological transformation of aggregates consisting of N_1 and N_2

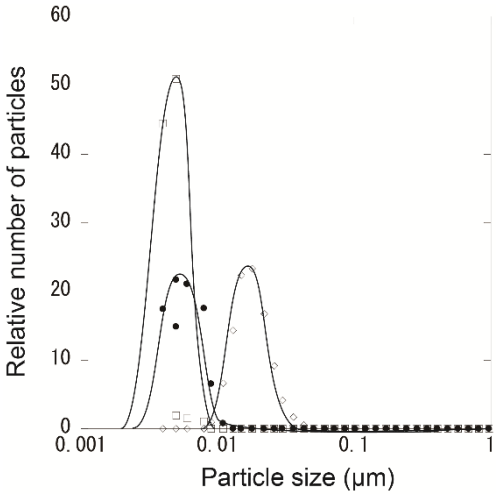

Figure S11. DLS distribution of micelles prepared from N_1 and N_2, separately (●for N_1, □ for N_2), and from a mixture of both (◇ for N_1 and N_2) obtained 30 min after addition.

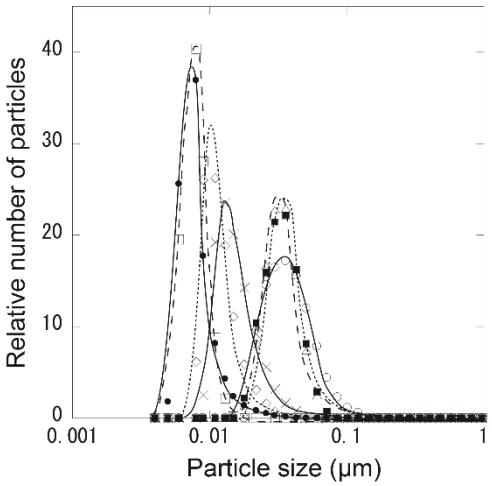

Figure S12. Time course of the size distribution of molecular aggregates formed in the aqueous dispersion of the equimolar mixture of N_1 and N_2 (10 mM for each) measured by the DLS method. —●— 0.5 h; - -□- - 1 h; ···◇··· 1.5 h; —×— 2 h, - -△- - 6 h, ···■··· 12 h, and —○— 120 h after

mixing.

The diameter of micelles formed from an equimolar mixture of amphiphiles $\mathbf{N_1}$ and $\mathbf{N_2}$ is larger than those of individual amphiphiles. The result indicates formation of hybrid micelles. Time course of the size distribution of the hybrid amphiphilic aggregates of $\mathbf{N_1}$ and $\mathbf{N_2}$ (10 mM for each) was measured by the DLS method at room temperature (Figure S12). This time period corresponds to a conversion of ca. 20% from $\mathbf{N_1}$ and $\mathbf{N_2}$ to **V**. The diameter of aggregates gradually grew larger than 10 nm in 1 h (conversion of ca. 35%) and eventually became 70 nm after 6 h (conversion of ca. 80%), reaching the maximum size. This indicates that the micelles spontaneously transformed into large aggregates, the size of which, however, remained almost constant even after a long time period. The transformation of transient structures from $\mathbf{N_1}$ and $\mathbf{N_2}$ to micron-sized granular aggregates could not be detected by DLS measurements probably because of the rapid formation of micron-sized granular aggregates associated with the accumulation of **V** during the measurement time (30 min).

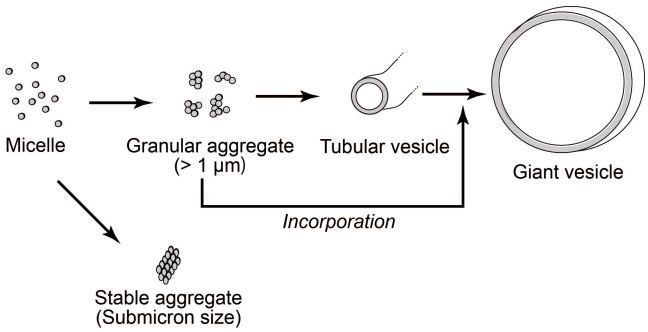

Figure S13. Schematic of morphological transformation from micelles to GV through granular aggregates and tubular GV and to submicron-size aggregates. Stable submicron-size aggregates detected by DLS were also formed through a minor route.